IOP Publishing Superconductor Science and Technology
Supercond. Sci. Technol. 32 (2019) 075007 (12pp) https://doi.org/10.1088/1361-6668/ab13d9

Effect of magnetic sheath on filament AC losses and current distribution in MgB_2 superconducting wires: numerical analysis

Y Nikulshin[1], **Y Yeshurun and S Wolfus**

Department of Physics, Institute of Superconductivity Bar-Ilan University, Ramat-Gan 52900, Israel

E-mail: yasha.nick@gmail.com

Received 18 January 2019, revised 24 March 2019
Accepted for publication 27 March 2019
Published 6 June 2019

Abstract

Finite element method (FEM) analysis is employed to study and compare AC losses in a wide frequency range in two MgB_2 superconducting wires in self-field and in the presence of external AC field. The modelled wires, of the same external dimensions, are mono- and 36-superconducting filaments embedded in either magnetic Monel or a nonmagnetic metallic wire sheath. We demonstrate that in a multifilamentary wire in self-field the Monel sheath serves as a 'pole piece' at the filament outer surface and alters local magnetic fields, current flow and AC losses distribution within the filament. In comparison with the nonmagnetic sheath with the same electrical conductivity, AC current in the wire with the magnetic sheath penetrates significantly deeper into the filaments and AC losses in the filament and in the magnetic sheath increase significantly. In contrast, the symmetry of the monofilament wire makes the current and loss distributions in the filament practically indifferent to the sheath composition. Still, losses in the magnetic sheath are much higher than in the nonmagnetic sheath due to increased flux dynamics. The application of DC current, on which the AC current is superimposed, sharply reduces the AC losses in the magnetic sheath material due to the drop in its permeability. Filament losses are also reduced in the presence of DC current, but to a much lesser extent. Results also show that in the kHz frequency range, the magnetic permeability of the sheath increases the skin effect in both the wire and filaments complex. As a result, at such frequencies, a significant portion of the current is carried by the metallic part of the wire instead of the superconductor, contributing to a further increase in losses. The analysis also shows that in the presence of external AC magnetic field, the Monel can provide magnetic shielding for inner filaments, thus reducing coupling effects between filaments. However, if magnetically saturated by the DC current, the Monel behaves quite similarly to a nonmagnetic sheath.

Keywords: MgB_2, AC losses, superconducting magnetic energy storage, finite element method

(Some figures may appear in colour only in the online journal)

1. Introduction

Superconducting wires and coils used in high-current applications, such as superconducting magnetic energy storage (SMES) and high-voltage direct current (HVDC), are often exposed to small AC current ripples at frequencies in the 10^4 Hz regime, resulting from pulse width modulation (PWM) control algorithms [1–4]. These AC ripples can induce significant AC losses, generating heat that falls as an extra load on the cryogenic system, increasing dramatically the cost of the device [2, 5–9]. In addition, excessive AC losses in the superconducting wires is a major factor in increasing the device instability and failure risk.

AC losses in superconducting materials are a well-studied phenomenon [10–12]. Superconducting wires, especially those with a magnetic sheath, are less explored because of the increased complexity due to the nonlinear magnetic nature of the filaments and the sheath and their mutual coupling [13–16]. Moreover, most studies of AC losses in superconducting wires

[1] Author to whom any correspondence should be addressed.

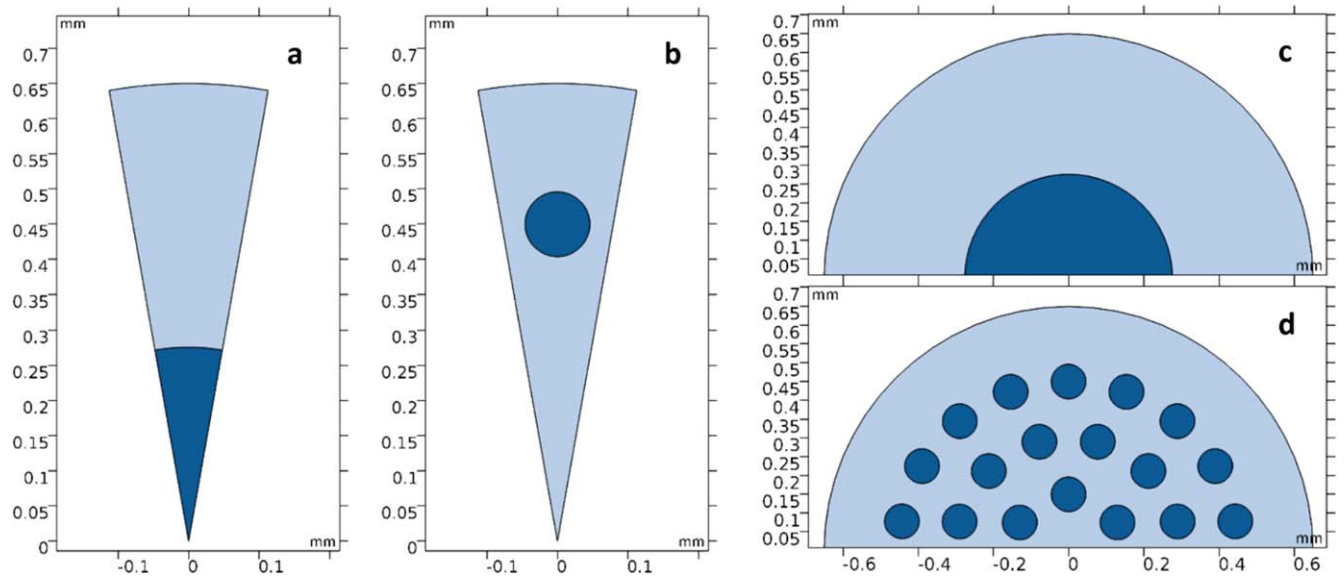

Figure 1. Wire topology of the model. Dark blue—superconducting area, light blue—metallic matrix. (a) Monofilament in self-field; 1/18 of the wire is shown in the figure and used for simulation. (b) Outer layer filament of the multifilament in self-field, 1/18 of the wire is shown in the figure and used for simulation. (c) Monofilament in external field, ½ of the wire is shown in the figure and used for simulation. (d) Multifilament in external field, ½ of the wire is shown in the figure and used for simulation.

focus on relatively low frequencies, of up to several hundred Hz [17–20]. In this work we use finite element method (FEM) modelling to analyze the AC losses in frequencies of up to 12.8 kHz, in two MgB_2 superconducting wires composed of a monofilament and 36-filaments embedded in magnetic (Monel, 70% Ni—30% Cu) and nonmagnetic metallic wire sheaths. The simulations show clearly that the total AC losses depend strongly on the magnetic properties of the wire matrix and sheath. In particular, the eddy currents in the Monel matrix are enhanced [13, 14], and its high permeability changes the magnetic field penetration pattern inside the superconducting filaments, contributing to additional hysteresis loss in the superconducting material itself.

This paper is organized as follows. In section 2 we describe the parameters used in the model for both the multi- and monofilament superconducting wires. We then analyze the losses in self-field in wires carrying AC current only. Multi- and monofilament wires are analyzed in sections 3 and 4, respectively. The same wires carrying AC current superimposed on a 40 A DC current are analyzed in section 5. In section 6 we analyze the losses of wires placed in external AC magnetic field. Finally, in section 7 we summarize the insights learnt from our simulations.

2. Model details

Two different topologies of a typical round wire with superconducting filament(s) have been compared in terms of their AC losses. Both wires have an outer diameter of 1.3 mm and they are composed of either a monofilament or 36-filaments, surrounded by either magnetic Monel or a nonmagnetic sheath. The radius of the monofilament is 0.276 mm and each of the 36 filaments has a radius of 0.046 mm, resulting in the same total superconducting cross section area of 0.15 mm^2, 18% of the total wire cross section. The wires were simulated under two different scenarios. First, the wire is in a self-field state, carrying either AC current or DC with superimposed AC currents. The AC current of 8 A_{rms} was chosen to be within the range used in previous experiments [13, 14], while convenient and sufficient for modelling yet far from the critical current. This case is representative of cables and current leads in general use. The second scenario represents the case where the modelled wire is part of a coil. Every winding of the coil experiences a transverse magnetic field produced by the coil itself. To mimic these conditions without simulating the whole coil, the wire is placed in an external magnetic field generated by an additional solenoid. The transverse magnetic field produced by the solenoid is in phase with the current in the modelled wire, exactly as if the wire was part of the coil. In this case, the transverse magnetic field breaks the circular symmetry of the self-field state and leads to a totally different loss profile. The DC bias current used in both cases is either zero or 40 A. It was experimentally proven [13] that this current is enough to saturate the Monel and reduce dramatically the effects related to the magnetic properties of the Monel.

The finite element models of the wires, based on H-formulation [21], have been built with commercially available software package COMSOL Multiphysics. The electrical behavior of the superconducting material is described by the E-J power law [22]. The sheath material resistivity used for the simulation is the measured resistivity of Monel at 10 K, 3.65 $\times$ 10^{-7} $\Omega\,m^{-1}$. For the magnetic matrix we take a field-dependent permeability $\mu_r = 1 + c_1(1 - e^{--H/c_2})/H)$ with $C_1 = 155\,600$ m A^{-1} and $C_2 = 905$ m A^{-1} and H, in units of A m^{-1}, is the magnetic field. The nonmagnetic material is represented by $\mu_r = 1$.

The wires are modelled as infinitely long in 2D space, assuming fully coupled filaments (without twist pitch). The

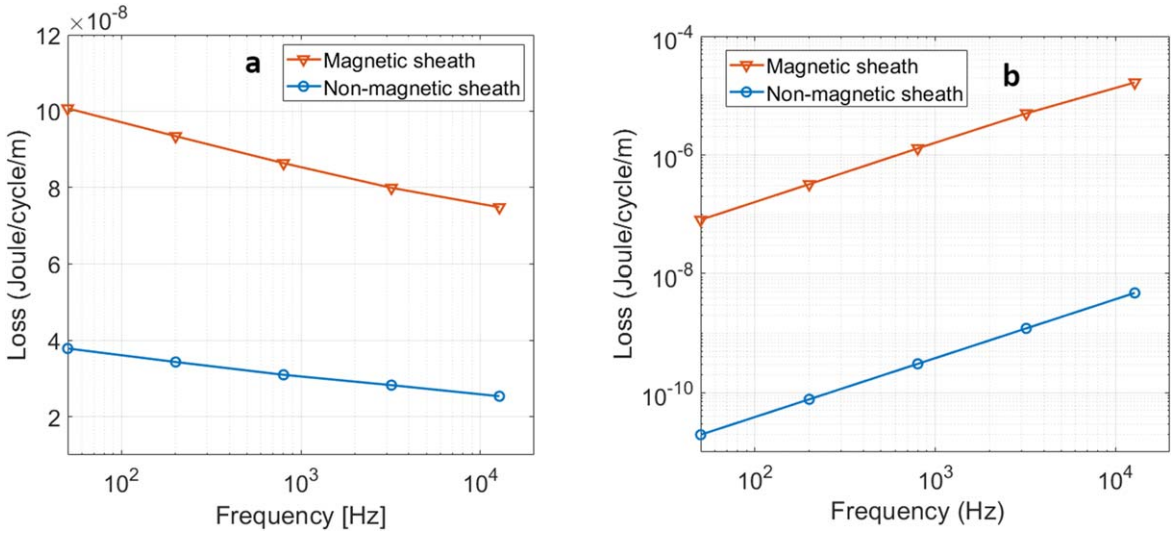

Figure 2. (a) Filaments loss (J/cycle/m) versus frequency of multifilamentary wire in self-field without DC bias in nonmagnetic sheath (blue open circles) and in magnetic sheath (red stars). (b) Sheath loss versus frequency (J/cycle/m) in nonmagnetic sheath (blue) and magnetic sheath (red).

Table 1. Model parameters.

Critical current density	5×10^8 A m^{-2}
n-Value	30
Characteristic voltage, E_0	1 μV cm^{-1}
Wire diameter	1.3 mm
Wire length	60 mm
Number of filaments	1, 36
MgB_2 fraction	18%
Frequencies, f	50, 200, 800, 3200, 12 800 Hz
AC current amplitude	8 A RMS
DC current	0, 40 A

multifilamentary wire has 18 filaments on its outer layer. In self-field and relatively small current amplitudes, the current does not fully penetrate the outer layer of the filaments and uncoupled and coupled filaments behave similarly. To save computational time, only 1/18 of the wire was calculated with applied periodic boundary conditions on the sector boundaries, as shown in figure 1. Thus, in the multi-filamentary wire, only the outer layer of filaments was modelled. The inner layers are totally screened from magnetic field and currents. This approach holds only for the self-field scenario. When the wire is in external field, the model makes use of the two-fold symmetry, namely 1/2 of the wire was computed (figure 1).

In self-field and zero DC bias current, only two cycles of the AC current are enough to reach the steady state behavior of the losses. When DC current is added to the AC current, an exponential decay of superconducting losses occurs because of the initial DC current charging. In this case, at least 15 cycles are required to reach steady state waveforms. The energy loss is calculated by both time and spatial integration of $J \cdot E$ over superconducting and metallic domains independently, during the last period of the AC current, namely $\int_0^T \left(\int J \cdot E \mathrm{d}S \right) \mathrm{d}t$. The model parameters are presented in table 1.

3. Self-field, multifilament

In this section, wires in self-field configuration are analyzed. Figure 2 shows a dramatic influence of the Monel ferromagnetic properties on the losses of the superconducting filament(s).

Losses in the superconducting filaments (figure 2(a)) is shown to increase by a factor of approximately three. In both cases, higher frequencies tend to reduce the losses. This is because part of the current flows in the metallic sheath instead of the filaments. This point is discussed further below.

The frequency dependence of the losses in the metallic sheath is presented in figure 2(b). The main loss mechanism in the metallic sheath of a superconducting wire is eddy currents induced by alternating magnetic field. The high magnetic permeability of the Monel is responsible for higher magnetic flux dynamics, resulting in an increase in the losses by about four orders of magnitude.

Figure 3 exhibits a momentary analysis of the multi-filamentary wire simulated in self-field at the peak of 8 A_{rms} in a selected frequency of 200 Hz. Clearly, the presence of magnetic material around the filament alters the magnetic flux density distribution, not only in the magnetic material itself but inside the superconducting filament as well. The scales in figures 3(a) and (b) are adjusted to the intensity of the magnetic field to have a better visualization of the effect. The magnetic sheath serves as a 'pole piece' and concentrates the magnetic flux on the outer edge of the filament, resulting in higher flux dynamics. More flux enters the superconductor through smaller areas where the total integration of the flux time-derivative over filament volume is higher for the magnetic sheath wire, hence the increased losses. Current

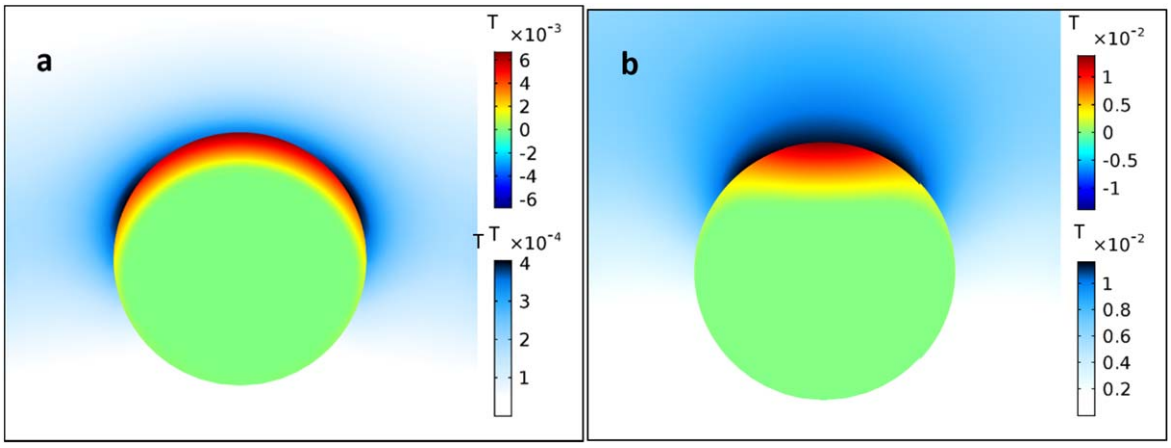

Figure 3. Magnetic field distribution (T) at 200 Hz at the peak of current (8 A_{rms}) for (a) nonmagnetic sheath, (b) magnetic sheath. The upper, red-blue scale is for the area inside the filament. The lower, blue-white scale is for the sheath.

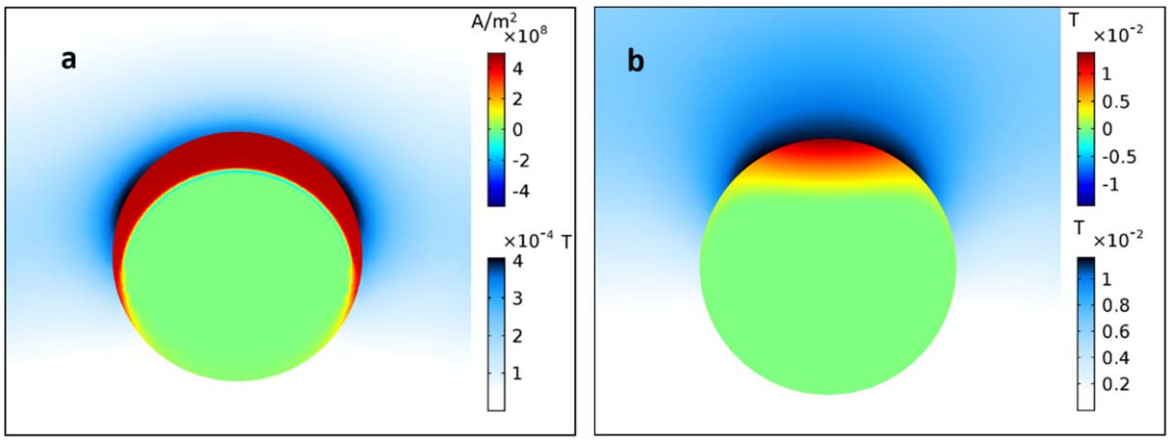

Figure 4. Current density (red-blue color scale) in a representative outer filament and magnetic field (blue-white color scale) in the matrix for (a) nonmagnetic sheath, (b) magnetic sheath. The figure describes the current and the field for 200 Hz at the current peak (8 A_{rms}).

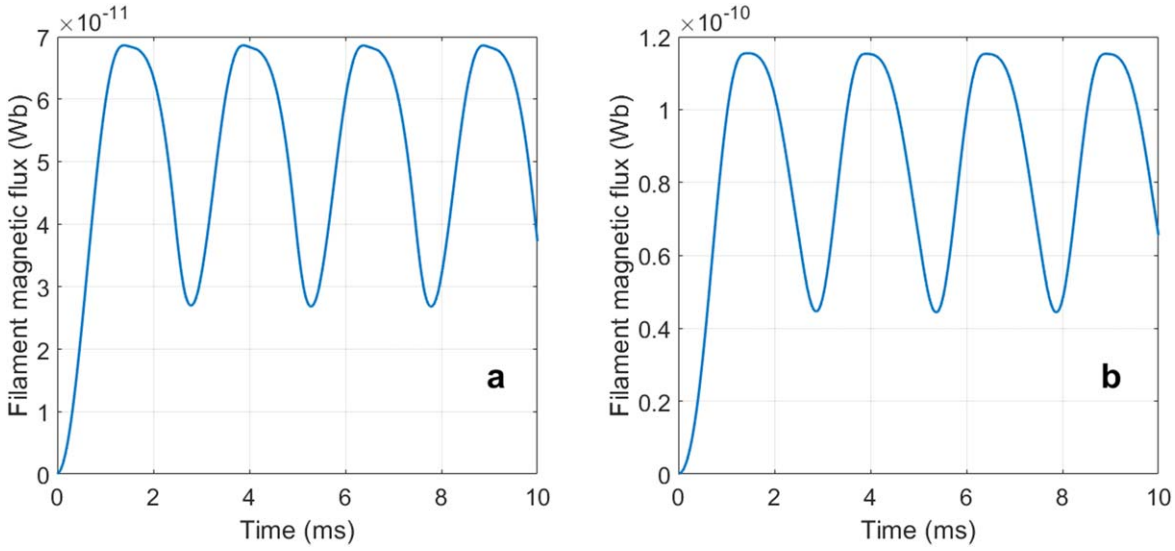

Figure 5. Flux penetration to the filament of multifilamentary wire in self-field produced by 8 A_{rms} at 200 Hz without DC bias. (a) Nonmagnetic sheath, (b) magnetic sheath.

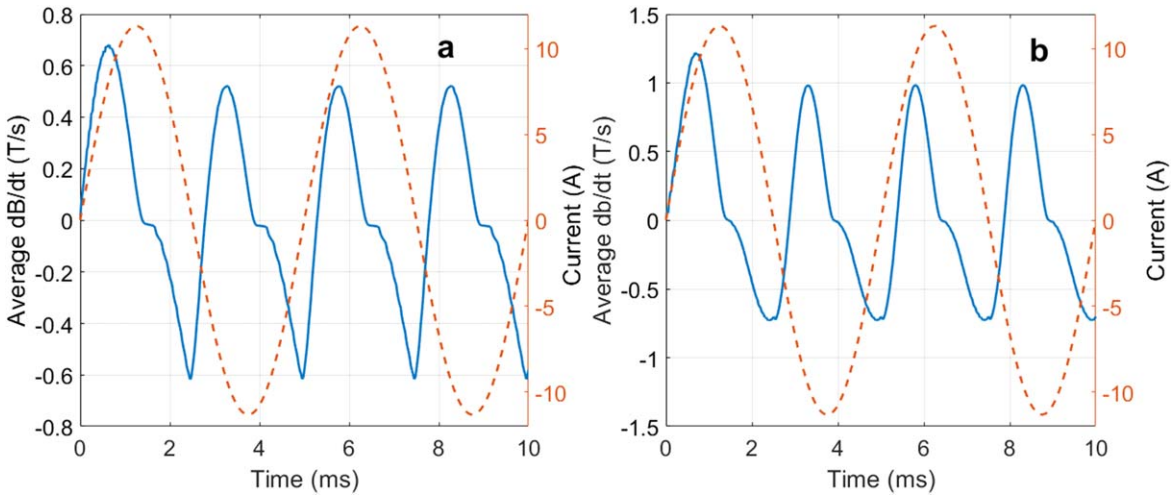

Figure 6. Average of dB/dt over the filaments of multifilamentary wire in self-field at 8 A_{rms} 200 Hz without DC bias. (a) Nonmagnetic sheath, (b) magnetic sheath.

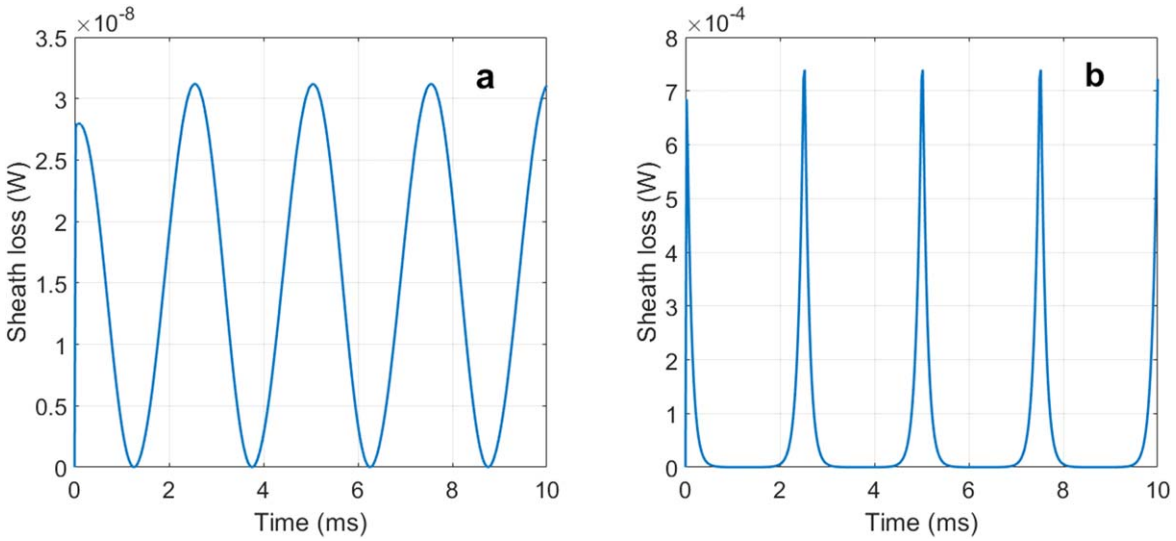

Figure 7. Momentary loss in metallic sheath of multifilamentary wire at 8 A_{rms} at 200 Hz without DC bias. (a) Nonmagnetic sheath, (b) magnetic sheath.

density distribution in the filament is also affected by the change in the surrounding magnetic profile. Like the magnetic field, the current is also concentrated near the edge of the filament (figure 4).

Figure 5 shows the total magnetic flux density integrated over the filament cross section, at maximum current amplitude of 8 A_{rms} at 200 Hz, for both magnetic and nonmagnetic sheaths. The Monel sheath forces ~70% more magnetic field to penetrate the filaments in self-field. The magnetic field is also more concentrated on the edge of the filament (figure 3).

These findings imply that local energy loss distribution results in a more localized heating that can lead to a hot spot. The presence of the magnetic sheath increases the filament loss by a factor of ~2.8 inside the filament and the sheath loss by a factor of $\sim 10^4$. All the magnetic flux in the model is produced by the AC current in the wire, therefore if more flux enters the filament more flux leaves it every cycle. Figure 6 shows the flux time-derivative, $\frac{1}{S}\int\left(\frac{d|B|}{dt}\right)ds$, averaged over the filaments. The current waveform is plotted in figure 6 in orange for a better visualization and easier analysis. The frequency of the flux time-derivative waveform is double the current frequency, because the calculation considers absolute value of flux, regardless of the direction. There is a small step-like feature at every maximum of the current, where the flux changes trend. Values of dB/dt are higher by ~70% in the Monel wire and the waveform is less symmetric around the zero line. This can probably be attributed to the nonlinear nature of magnetic properties of the Monel.

The nonsinusoidal behavior of the dissipated power in the magnetic sheath (figure 7(b)) originates from the nonlinear magnetic properties of the Monel. Each time the AC current crosses zero, the magnetic field in the wire is very low

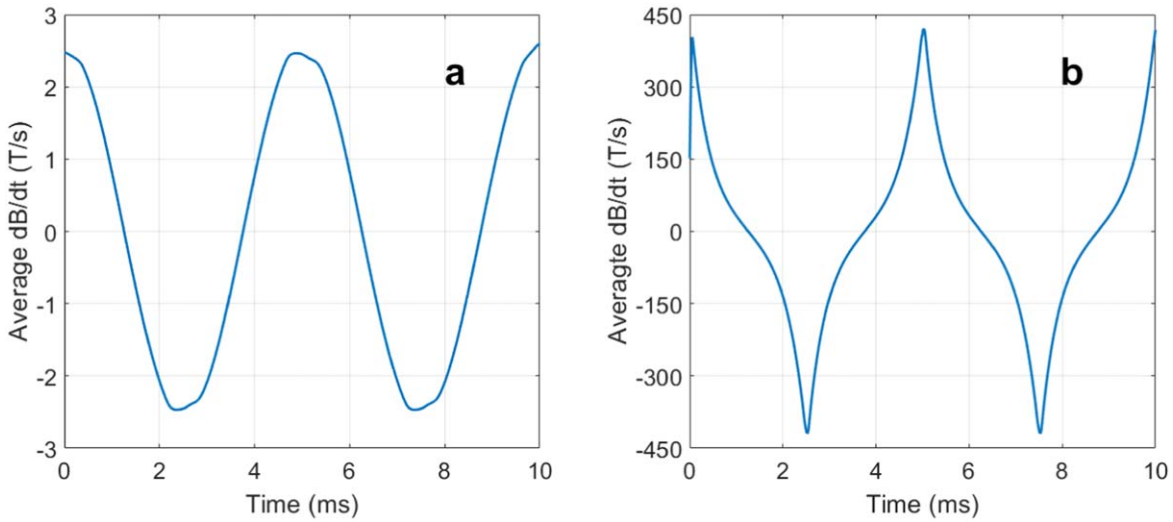

Figure 8. Average of dB/dt over the sheath of multifilamentary wire in self-field at 8 A_{rms} at 200 Hz without DC bias. (a) Nonmagnetic sheath, (b) magnetic sheath.

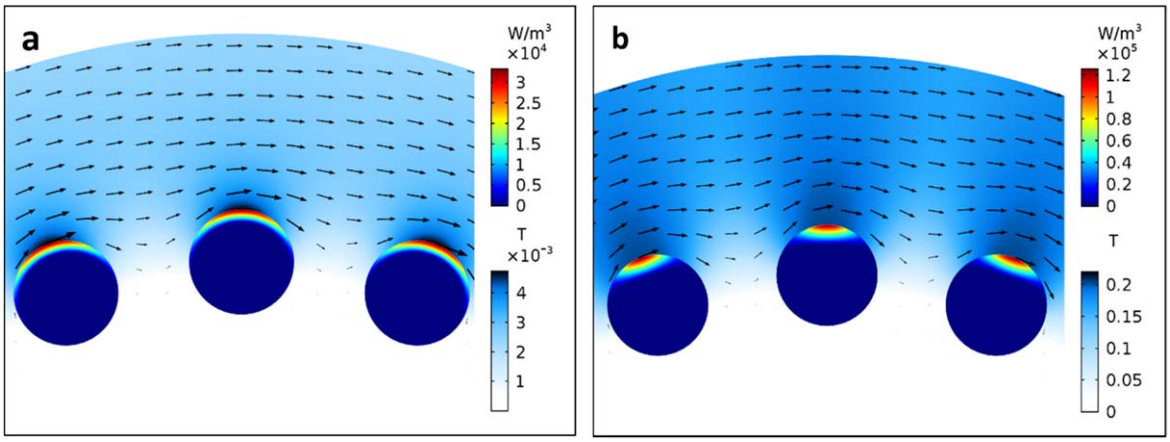

Figure 9. Loss distribution in filament of multifilamentary wire in self-field at $t = 81$ ms at A_{rms} at 200 Hz without DC bias. (a) Nonmagnetic sheath, (b) magnetic sheath. The upper and lower scales refer to volumetric loss density and magnetic flux density respectively. The arrows show magnetic flux direction.

and, as a result, the Monel has its highest permeability. At these times, dI/dt is maximal, inducing the highest eddy currents in the Monel.

The time derivative flux in the sheath averaged over the sheath area is depicted in figure 8. The magnetic properties of the Monel increase the flux variation by two orders of magnitude and the momentary losses by four orders of magnitude.

The energy loss density of the multifilamentary wire in self-field at 200 Hz without DC current, at $t = 81$ ms, is depicted in figure 9. At this point in time the losses are near their maximum in the period. Here again, we see strong evidence for the influence of the outer sheath on the losses within the filaments. As expected, the loss density follows the magnetic field penetration profile. Although the area where most of the losses are concentrated is smaller for the magnetic sheath wire, the peak value of the losses in this case is about four times higher than for the nonmagnetic wire, resulting in higher overall losses.

At high frequencies, part of the transport current flows in the metallic section of the wire rather than in the superconducting filaments, even for the case of the nonmagnetic sheath. This happens in every conductor due to skin effect. The effect is amplified when magnetic Monel is being used and/or as frequency increases. Figure 10 shows the distribution of current between the filaments and sheath, in both scenarios, at 12.8 kHz. Apparently, for the Monel case, the current in the Monel peaks near the point where the total current in the wire crosses zero. At this point the Monel permeability is the highest, resulting in a stronger skin effect. With the increase in the total current, more of the Monel section is being magnetically saturated, thus taking less current. This change in the permeability of the Monel not only

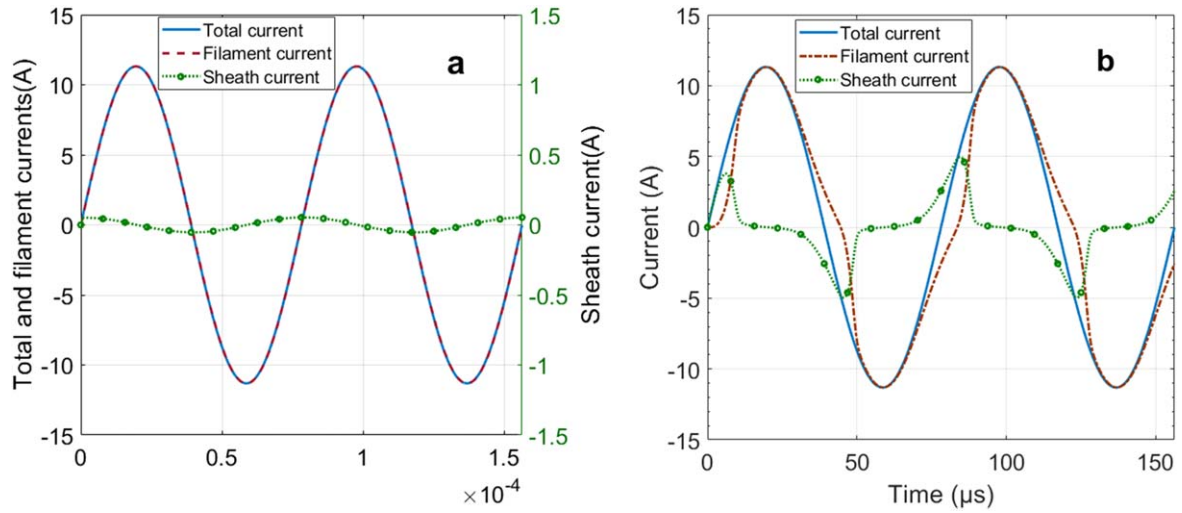

Figure 10. Current waveforms at 12.8 kHz of the total current (blue), filament current (green), and metallic sheath current (red). (a) Nonmagnetic sheath, (b) magnetic sheath.

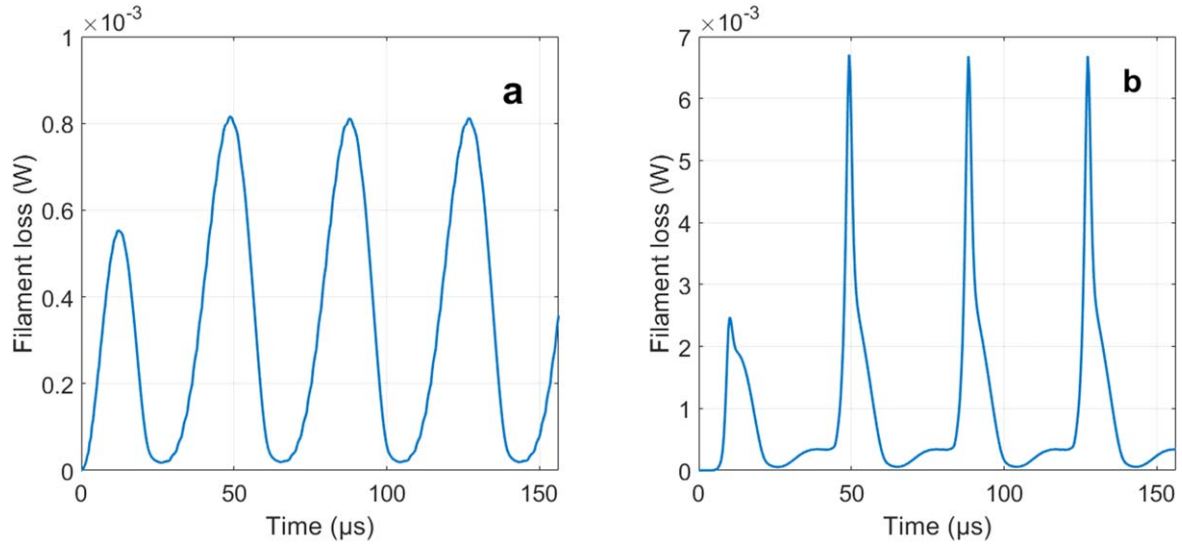

Figure 11. Momentary loss in the filament of multifilamentary wire in self-field at 12.8 kHz without DC bias. (a) Nonmagnetic sheath. (b) Magnetic sheath.

increases the skin effect and shares more current with the superconductor, but also increases flux dynamics and by doing so increases eddy currents losses in the sheath. On the other hand, sharing part of the current between Monel and the superconductor reduces the current in the filaments hence the superconducting losses. Also evident in figure 10(b) is a phase shift between the filament and sheath currents. This is an intrinsic property of induced currents since their source is the time derivative of the magnetic field.

The sudden transition of the Monel between nonsaturated and saturated states causes a very rapid flux change in the filament (figure 12(b)). At the saturation point of the Monel, which happens around $t = 0.5 \times 10^{-4}$ s, i.e. when the current reaches 8 A, all the current flowing in the sheath (figure 10(b)) is rapidly discharged, causing additional flux penetration into the filament. This transient causes a loss spike in the filament (figure 11(b)). This behavior is totally absent with the nonmagnetic sheath (figure 11(a), figure 12(a)).

4. Self-field, monofilament

For the monofilament wire in self-field, the filament losses are similar for the magnetic and nonmagnetic sheath wires (figure 13(a)) except at the highest frequency (12.8 kHz). The magnetic sheath increases the skin effect and causes more current to flow in the sheath and less in the filament (figure 13(b)). This current sharing phenomenon is even more pronounced for the monofilamentary wire than for the multifilamentary wire described above. Here the filament is carrying less current. A possible explanation is that the radius of the monofilament is smaller than the radius of the outer layer

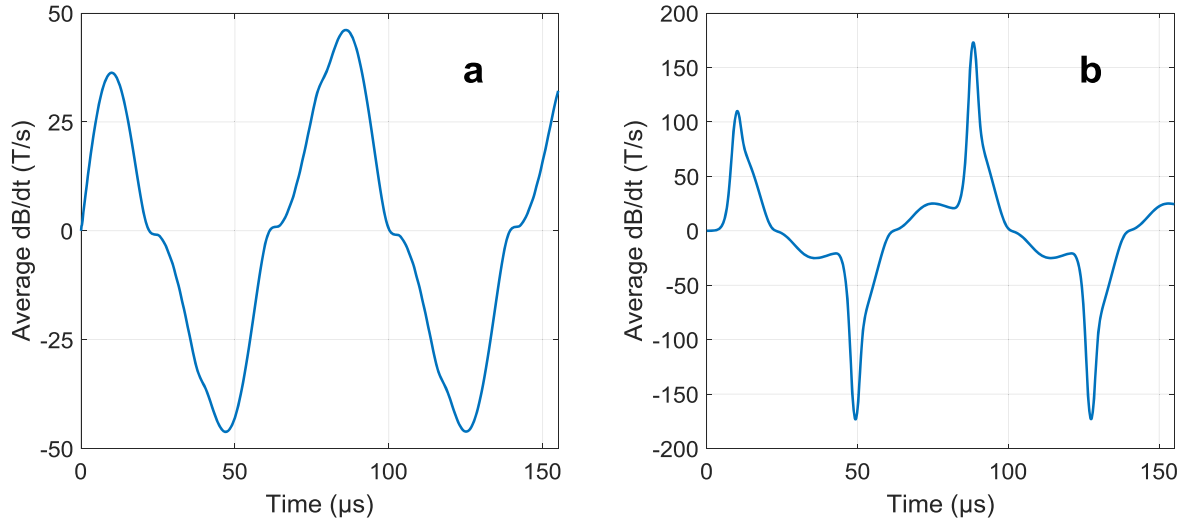

Figure 12. Average of dB/dt over the filament of multifilamentary wire in self-field at 12 800 Hz without DC bias. (a) Nonmagnetic sheath. (b) Magnetic sheath.

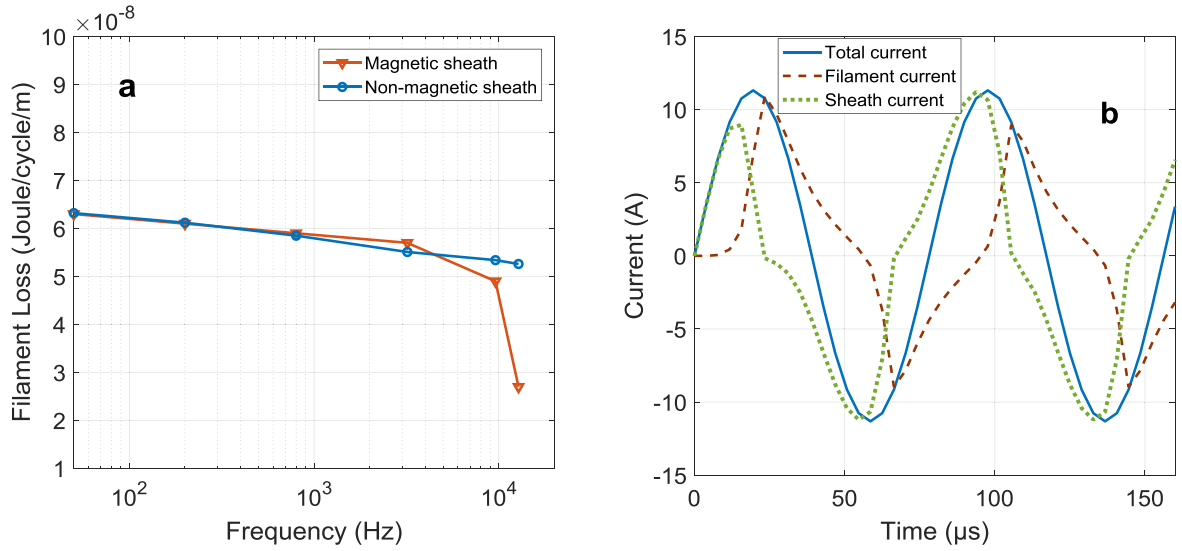

Figure 13. (a) Filament losses versus frequency for monofilamentary wire with nonmagnetic sheath (blue) and magnetic sheath (red). (b) Current waveforms for total current (blue), filament current (green) and sheath current (red) for monofilamentary wire with magnetic sheath at 12.8 kHz 8 A_{rms} without DC bias.

of filaments in multifilamentary wire. For the total wire diameter this makes the sheath thicker around the filament. This increases the current required for Monel saturation and increases the skin effect even further. Hence the metallic losses in monofilament are significantly higher than in multifilamentary wire for the same case (figure 14). The loss ratio of the sheath losses between magnetic and nonmagnetic sheaths remains the same for monofilamentary and multifilamentary wires.

5. DC bias

In this section we analyze the AC losses in the common case where AC current is superimposed on DC current. Specifically, we select here 40 A DC and 8 A_{rms} AC currents, to match the values in our previous experimental studies [13, 14]. For this relatively low DC bias value the current flows in the outer filament layer without fully penetrating the filaments. The analysis of monofilamentary wire shows that there is virtually no difference in filament loss between magnetic and nonmagnetic metals surrounding the filament, see triangles and circles in figure 15. As we show here, (see the 'x' and asterisk markers in the figure) this is not the case for a multifilamentary wire, where the filament losses are significantly higher when the sheath is magnetic.

To further investigate this difference, we analyzed the magnetic field distribution in the sheath. The magnetic field generated by the DC current is insufficient to fully saturate the Monel around the filaments. Instead, it creates areas with high and low permeability. The distribution of the permeability of the magnetic sheath in multifilamentary wire is shown in

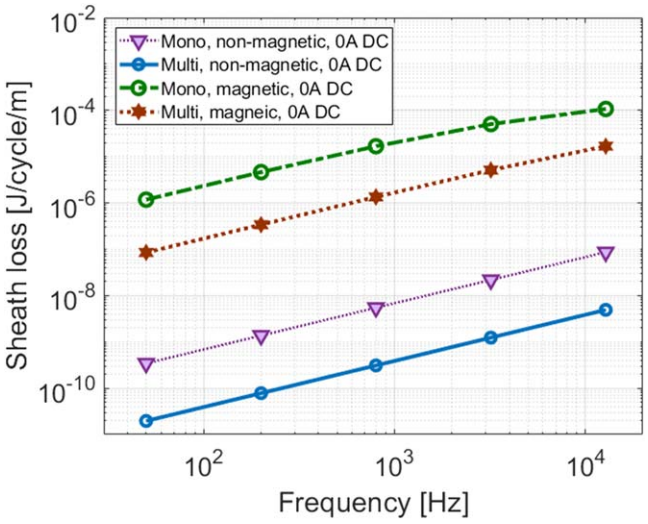

Figure 14. Sheath loss versus frequency (J/cycle/m) without DC bias.

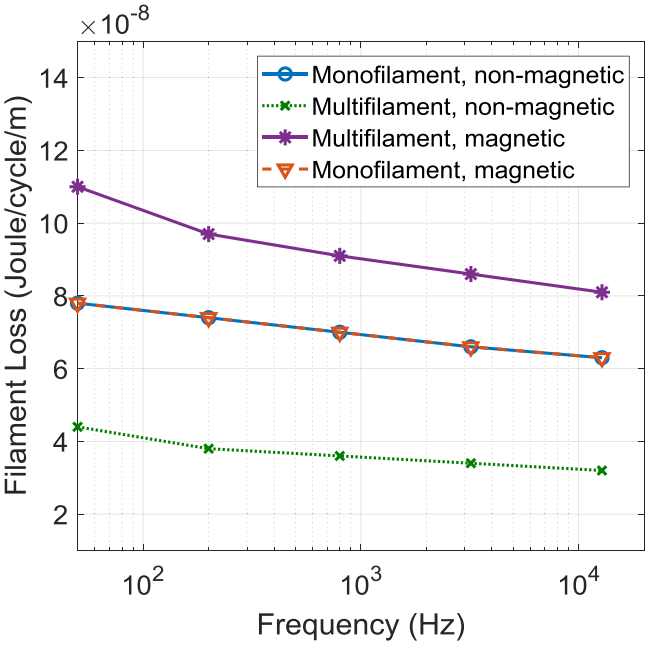

Figure 15. Filament losses versus frequency with 40 A DC current for magnetic and nonmagnetic sheath wires.

figure 16 for a temporary snapshot taken at the maximum peak current value of 51.3 A (40 A DC + 8 A_{rms}). The division of superconducting material to filaments produces gaps in between successive filaments where the magnetic field is lower than at the far edge of the filaments, although the outer layer of filaments is filled with superconducting current. The concentration of magnetic field leads to higher $d\phi/dt$ compared to filaments with nonmagnetic sheath. Significantly higher DC currents can saturate the area around the outer layer of filaments, but then the inner layer of filaments experiences the same problem of nonsaturated Monel, however, with a smaller number of filaments. This can explain the relatively slow reduction of losses with increasing DC current [13].

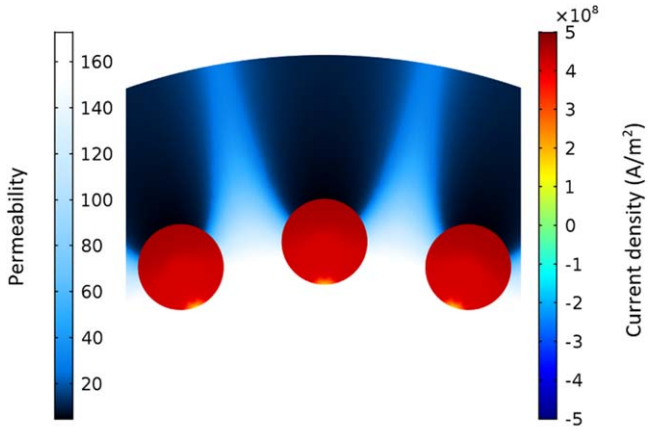

Figure 16. Distribution of the permeability in multifilamentary wire with Monel sheath at peak current, i.e. 40 A DC + 8 A_{rms}, 51.3 A in total (color code at left hand side) and distribution of the current density inside the filaments (color code at right).

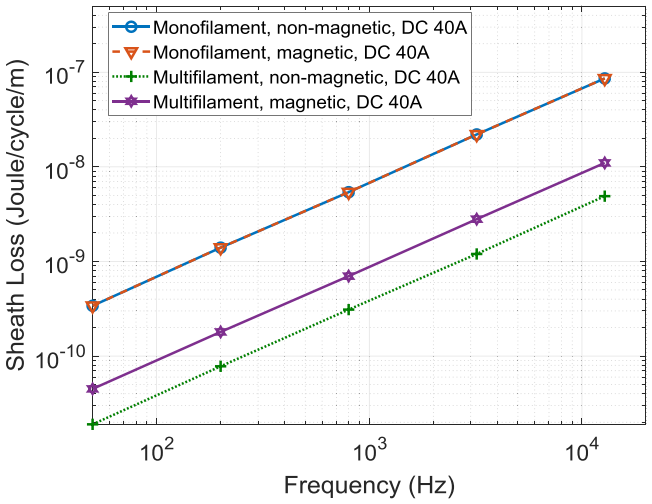

Figure 17. Sheath loss versus frequency (J/cycle/m) at 8 A_{rms} with 40 A DC bias.

As seen in figure 17, the sheath losses in monofilamentary wire are very similar in both magnetic and nonmagnetic sheath materials when 40 A DC current is added to 8 A_{rms} AC, and are higher than in the case of the multifilamentary wire. Since for mono- and multifilamentary wires the superconducting cross section area and the diameter of the wire are the same, the single filament of the monofilamentary wire is constricted at the center of the wire. The amount of sheath material around the filament region is thus larger, hence the eddy currents loops are larger and, consequently, the losses are larger.

6. External magnetic field

Most superconducting applications are coil-based. Inside a coil, every single winding experiences the influence of the other windings in the coil. From the point of view of a single winding, the magnetic field it experiences is always

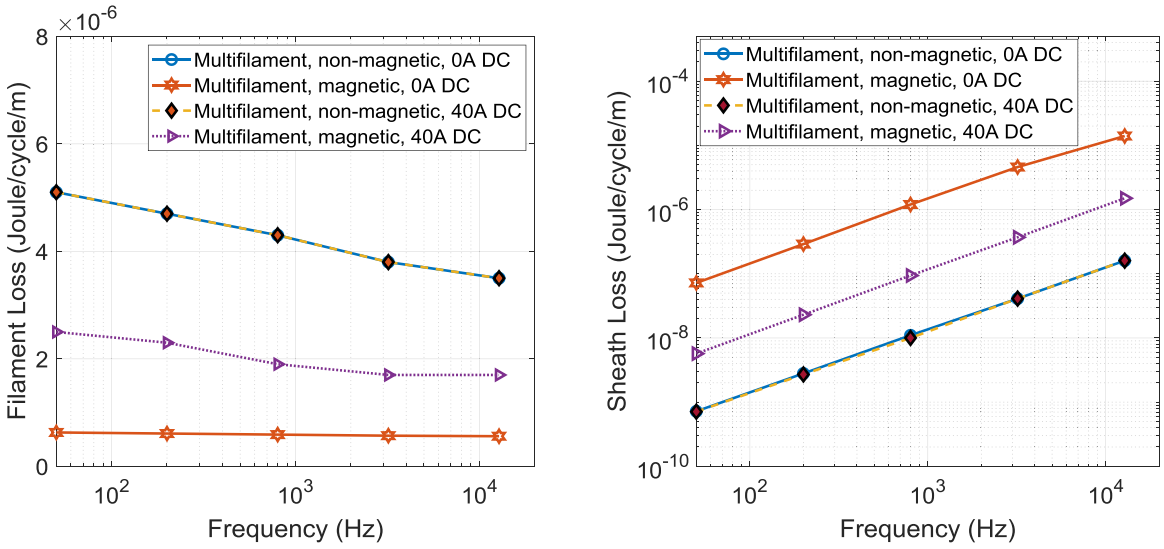

Figure 18. Loss (J/cycle/m) of multifilamentary wire in external field. (a) Filaments. (b) Sheath.

transverse. The circular symmetry, as in the above discussed cases, is no longer valid. This scenario is modelled to represent the losses inside a wire when it is part of a coil. To model it, first we added a long solenoid of 10 windings around the wire oriented to create transverse field on the wire. Each winding of this additional solenoid carries the same DC and AC currents as modelled for the stand-alone wire. The current in this solenoid is in phase with the current in the modelled wire itself. The infinite 2D model implies fully coupled filaments. The selected coil geometry generates an external field of 7.4 mT A^{-1}. In this scenario, the alternating external magnetic field induces current both in the superconductor and in the sheath to expel the magnetic field.

As seen in figure 18, in the presence of external magnetic field the difference in filament losses between magnetic and nonmagnetic sheaths, for both zero DC and 40 A DC bias, is smaller than in self-field (figure 15). Surprisingly, the lowest loss values are obtained for the magnetic sheath wire without DC bias (see hexagrams in figure 18(a)). These results are in contrast to the self-field case (figure 2(a)), where the exact same wire configuration model exhibited the highest loss values. To explain this result, we note that the magnetic Monel is shielding the magnetic field in the central part of the wire and therefore currents flow in this area within the superconducting filaments. In figure 19, a snapshot of such wire at the peak AC current amplitude of 11.3 A at 200 Hz is displayed. The right side of the wire carries positive critical current while filaments on the left side carry negative current. Due to lack of filament twisting the coupling between them is very strong, thus transversal AC magnetic field induces infinite current loops within the wire. In fact, most of the wire current is screening current rather than transport. Both wires with magnetic and nonmagnetic sheaths are subject to developing such currents. This coupling current is responsible for an increase of two orders of magnitude in filament losses compared to the self-field case for both cases. The sheath

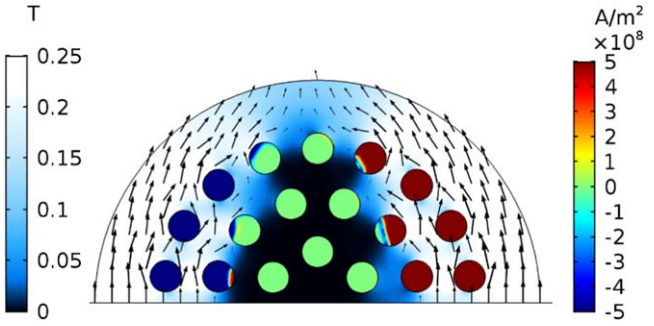

Figure 19. Field and current distribution in a multifilamentary wire with magnetic sheath in external field at peak AC current at 200 Hz, zero DC bias. The color coding is depicted in the left and right scales for the field and current, respectively.

losses, however, are higher because this shielding effect induces higher currents in the sheath as well.

Figure 20 displays the same scenario as in figure 19, but for a nonmagnetic sheath. As clearly seen in the figure, in this case the magnetic field fully penetrates the wire. All filaments take part in screening the AC flux variation of the external field to the extent that in some filaments, at the center of the wire, positive and negative currents coexist in the same filament. Since the matrix has low permeability, the flux time-derivative is lower, thus screening currents and losses are lower compared to the magnetic sheath case.

When DC current is added, the difference in superconducting filament loss diminishes (see orange hexagrams and purple triangles in figure 18(a)) because the external field is enough to partially saturate the Monel and thus reduces the shielding effect of the Monel. This is also evident in the sheath losses which become lower with 40 A DC current (figure 18(b)).

At the zero AC current point one can see a trapped flux between positive and negative currents in the filaments (red and blue areas). This unique distribution of current causes the

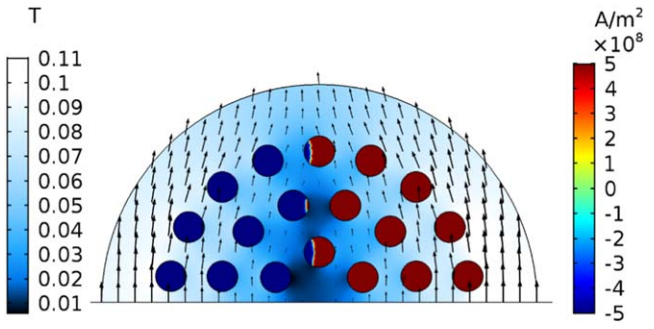

Figure 20. Field and current distribution in a multifilamentary wire in external field at peak current at 200 Hz, nonmagnetic sheath and zero DC bias. The color coding is depicted in the left and right scales for the field and current, respectively.

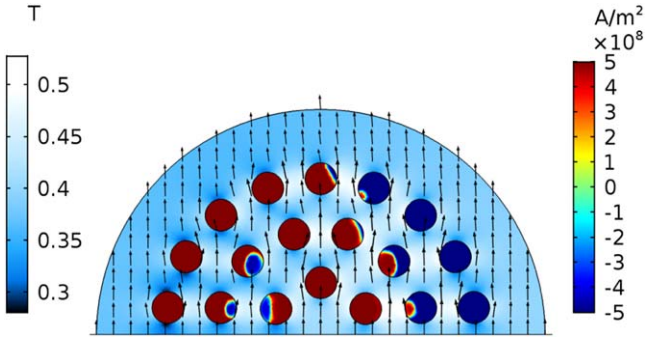

Figure 21. Field and current distribution in a multifilamentary wire with magnetic sheath in external field at zero AC current, and 40 A DC bias. The color coding is depicted in the left and right scales for the field and current, respectively.

local field between the filaments to be even higher than the applied external field (figure 21).

7. Summary and conclusions

Monofilamentary and multifilamentary wire topologies have been modeled with FEM for AC losses in self-field and external magnetic field.

Our results reveal the disadvantages of using a magnetic sheath for superconducting wires exposed to high-frequency switching, suggesting a need to redesign wires for applications such as SMES. In self-field, the high magnetic permeability of Monel alters the magnetic flux density distribution, both inside the magnetic material itself and in the superconducting filament (s). The magnetic sheath causes the magnetic field to concentrate at the edge of the outer filaments of multifilamentary wire, resulting in an increase in the losses not only in the sheath but also in the filaments. Although the area of the filament where most of the loss occurs is smaller, the peak value of the loss in this case is about four times higher than for the nonmagnetic wire, resulting in higher overall loss.

For the multifilamentary wire at frequencies above $\sim 10^3$ Hz, the eddy currents in the nonsaturated magnetic sheath dominate the filament losses and become the most significant heat source. These findings are in good agreement with results obtained experimentally [13, 14]. Upon decreasing permeability due to saturation, the eddy currents produced in the sheath decrease accordingly. In this case the relative reduction of loss in the sheath is higher than measured experimentally. This could be a result of magnetic hysteresis in the Monel which was neglected in our analysis.

The skin effect leads to current sharing between superconducting filaments and the metallic sheath reducing the losses in the filaments while dramatically increasing them in the sheath. A very rapid flux change in the filament, which generates momentary loss spikes, is caused by the transition of Monel from nonsaturated to saturated states and vice versa. Such localized dissipation might lead to hot spots in the wire and reduce the overall stability of the system.

In the monofilament wire, there is no difference in filament losses between the cases of magnetic and nonmagnetic sheaths. Due to the circular symmetry, the 'pole piece' effect which concentrates the field in the filament edges is absent, thus no increase in losses is observed in the superconductor. The losses in the sheath are much higher as expected in the case of magnetic Monel.

In the external magnetic field, the Monel partially shields the filaments, reducing the losses in them when no DC bias is applied. However, in this case the eddy currents losses in the sheath are increased. With DC current the external magnetic field deeply saturates the Monel resulting in quite similar behavior of losses in the filaments surrounded by either magnetic or nonmagnetic metal.

At low frequencies, due to strong filament coupling, the filament losses dominate in most cases where external field is applied. At high frequencies, sheath losses are similar or higher than filament losses. When the Monel is not magnetically saturated, it becomes the dominant source of AC losses. While in almost every superconducting coil the magnetic field is high enough to saturate the Monel, there will always be an area in the center of the coil where the field is very small. This area may behave as an undesired heat source, adding to the disadvantages of using a magnetic sheath in applications such as SMES, where the wires are exposed to AC current ripples.

Acknowledgments

This research was supported by the Ministry of Science Technology and Space, Israel.

ORCID iDs

Y Nikulshin https://orcid.org/0000-0001-7753-1334

References

[1] Marian A, Holé S, Lesur F, Tropeano M and Bruzek C E 2018 Validation of the superconducting and insulating components of a high-power HVDC cable *IEEE Electr. Insul. Mag.* **34** 26–36

[2] Liu D, Polinder H, Magnusson N, Schellevis J and Abrahamsen A B 2016 Ripple field AC losses in 10-MW wind turbine generators with a MgB_2 superconducting field winding *IEEE Trans. Appl. Supercond.* **26** 1–5
[3] Lahtinen V and Stenvall A 2013 The difficulty of modeling ripple field losses in superconductors using the eddy current model *IEEE Trans. Appl. Supercond.* **23** 4900505
[4] Bruzek C E, Ballarino A, Escamez G, Giannelli S, Grilli F, Lesur F, Marian A and Tropeano M 2017 Cable conductor design for the high-power MgB_2 DC superconducting cable project of BEST PATHS *IEEE Trans. Appl. Supercond.* **27** 1–5
[5] Hong Z, Ye L, Majoros M, Campbell M and Coombs T 2008 Numerical estimation of AC loss in MgB_2 wires in self-field condition *J. Supercond. Nov. Magn.* **21** 205–11
[6] Majoros M, Sumption M D, Susner M A, Tomsic M, Rindfleisch M and Collings E W 2009 AC losses in MgB_2 multifilamentary strands with magnetic and non-magnetic sheath materials *IEEE Trans. Appl. Supercond.* **19** 3106–9
[7] Shintomi T *et al* 2013 Design study of MgB_2 SMES coil for effective use of renewable energy *IEEE Trans. Appl. Supercond.* **23** 5700304
[8] Young E, Bianchetti M, Grasso G and Yang Y 2007 Characteristics of AC loss in multifilamentary MgB_2 tapes *IEEE Trans. Appl. Supercond.* **17** 2945–8
[9] Lahtinen V, Pardo E, Šouc J, Solovyov M and Stenvall A 2014 Ripple field losses in direct current biased superconductors: Simulations and comparison with measurements *J. Appl. Phys.* **115** 113907
[10] Norris W T 1970 Calculation of hysteresis losses in hard superconductors carrying ac: isolated conductors and edges of thin sheets *J. Phys. D: Appl. Phys.* **3** 308
[11] Carr W J 2014 *AC Loss and Macroscopic Theory of Superconductors* (Boca Raton, FL: CRC Press)
[12] Wang Y 2013 *Fundamental Elements of Applied Superconductivity in Electrical Engineering* (Solaris South Tower, Singapore: Wiley)
[13] Nikulshin Y, Wolfus S, Friedman A, Ginodman V, Grasso G, Tropeano M, Bovone G, Vignolo M, Ferdeghini C and Yeshurun Y 2018 Monel contribution to AC losses in MgB_2 wires in frequencies up To 18 kHz *IEEE Trans. Appl. Supercond.* **28** 1–6
[14] Nikulshin Y, Wolfus S, Ginodman V, Friedman A, Tropeano M, Grasso G and Yeshurun Y 2018 AC losses in MgB_2 wires and tapes in frequencies up to 18 kHz *IEEE Trans. Appl. Supercond.* **28** 1–4
[15] Sumption M, Collings E, Lee E, Wang X, Soltanian S and Dou S 2002 Reduction and elimination of external-field AC loss in MgB_2/Fe wire by *in situ* magnetic shielding *Phys. C Supercond.* **378–381** 894–8
[16] Kováč J, Šouc J, Kováč P and Hušek I 2015 AC losses of single-core MgB_2 wires with different metallic sheaths *Physica C* **519** 95–9
[17] Michael P C, Kvitkovic J, Pamidi S V, Masson P J and Bromberg L 2017 Development of MgB_2-cabled conductors for fully superconducting rotating electric machines *IEEE Trans. Appl. Supercond.* **27** 1–5
[18] Kovac P, Husek I, Kovac J, Melisek T, Kulich M and Kopera L 2016 Filamentary MgB_2 wires with low magnetization AC losses *IEEE Trans. Appl. Supercond.* **26** 1–5
[19] Sumption M D 2018 AC loss of superconducting materials in motors and generators for very high density motors and generators for hybrid-electric aircraft *2018 AIAA/IEEE Electric Aircraft Technologies Symp. AIAA Propulsion and Energy Forum* (American Institute of Aeronautics and Astronautics) (https://doi.org/10.2514/6.2018-5001)
[20] Escamez G, Sirois F, Lahtinen V, Stenvall A, Badel A, Tixador P, Ramdane B, Meunier G, Perrin-Bit R and Bruzek C-E 2016 3D numerical modelling of AC losses in multi-filamentary MgB_2 wires *IEEE Trans. Appl. Supercond.* **26** 1–7
[21] Brambilla R, Grilli F and Martini L 2007 Development of an edge-element model for AC loss computation of high-temperature superconductors *Supercond. Sci. Technol.* **20** 16–24
[22] Hong Z, Campbell A M and Coombs T A 2006 Numerical solution of critical state in superconductivity by finite element software *Supercond. Sci. Technol.* **19** 1246–52